Available online at www.sciencedirect.com
ScienceDirect
Journal of Power Sources 159 (2006) 323–327
JOURNAL OF POWER SOURCES
www.elsevier.com/locate/jpowsour

Short communication

Electrochemical and charge/discharge properties of the synthesized cobalt oxide as anode material in Li-ion batteries

Jing-Shan Do*, Chien-Hsiang Weng

Department of Chemical Engineering, Tunghai University, Taichung 40704, Taiwan

Available online 26 May 2006

Abstract

The electrochemical and charge/discharge behaviors of cobalt oxide prepared by the calcination of cobalt hydroxide were studied by the cyclic voltammetry (CV) and galvanostatical charge/discharge methods. The cyclic voltammograms of cobalt oxide containing 20% carbon black were correlated well with the results in the charge/discharge behaviors of Li/CoO batteries. A cathodic peak with potential of 0.5 V (versus Li/Li^+) in the first cycle of CV corresponded to the plateau with voltage of 1.0–0.8 V in the first discharge cycle of Li/CoO battery was deduced to be the reduction and decomposition of CoO particle to be the nano-sized Co and Li_2O. Both of the cathodic peak and the discharge plateau voltages were shifted to higher values in the following cycles due to the reduction of CoO particle from micro to nano-size.

Keywords: CoO; Electrochemical behaviors; Li/CoO battery; Charge/discharge properties

1. Introduction

Lithium-ion battery has been considered as a promising power source for the modern electronic applications due to its highest energy density among commercial rechargeable batteries. The high specific capacity is found for using the metal oxides as the anodic materials of lithium ion battery [1–4]. Co_3O_4 [5–9] and various vanadates [10–13] are also used as anodic materials in the lithium-ion batteries. Though the relative higher reversible specific capacities are found in these materials, however, the large irreversible capacity in the first cycle and fading rate are need to be improved for further applications. A new insertion–extraction mechanism different from the carbonaceous compounds or lithium-alloying processes is proposed by using, namely, nano-sized transition-metal oxides (MO, where M is Co, Ni, Cu or Fe) [5,7,14–18]. The reversible capacity of CoO is obtained to be 600–800 mAh g^{-1} in the room temperature [5,14,16]. However, CoO studied in the most of the investigations is the commercial products. In general, the electrochemical and charge/discharge characteristics of CoO used as the anodic material of lithium-ion battery would be affected by the particle size, morphology and crystallinity of CoO. Using the CoO synthesized by us as anode material of lithium ion battery, the effect of calcination temperature on the characteristics and charge/discharge properties of CoO was discussed in our previous paper [19].

CoO is prepared by the calcination of $Co(OH)_2$ precursor synthesized by the chemical precipitation. The electrochemical behaviors of CoO electrode was studied by cyclic voltammetry and compared with the results in charge/discharge process.

2. Experimental

$Co(OH)_2$ prepared by the chemical precipitation method was calcinated in a tubular oven under 99.995% N_2 atmosphere as described previously [19]. The crystallographic information, grain size and surface morphologies of the prepared CoO were analyzed by X-ray powder diffraction (XRD, Shimadzu XRD-6000) and SEM (Joel JSM-5400), respectively.

The cobalt oxide electrodes were made by scraping and pressing the paste prepared by mixing PVDF (poly(vinylidene fluoride)), CoO powder and NMP (*N*-methyl-2-pyrrolidinone) on Cu foil [19]. The thickness and loading of CoO dried in a vacuum oven at 120 °C for 2 h were measured to be 80–100 μm and 5.5–7.0 mg, respectively. The cyclic voltammograms of CoO electrode were measured with an electrochemical analyzer (CHI 604) in 1.0 M $LiPF_6$ EC–DEC (ethylene carbonate–diethyl carbonate, provided by FERRO) (v/v 1:1) electrolyte. Li/CoO coin cells were fabricated in a glove-box (VAC MO-5) filled with

* Corresponding author. Tel.: +886 4 23590262x114; fax: +886 4 23590009.
E-mail address: jsdo@thu.edu.tw (J.-S. Do).

0378-7753/$ – see front matter © 2006 Elsevier B.V. All rights reserved.
doi:10.1016/j.jpowsour.2006.04.054

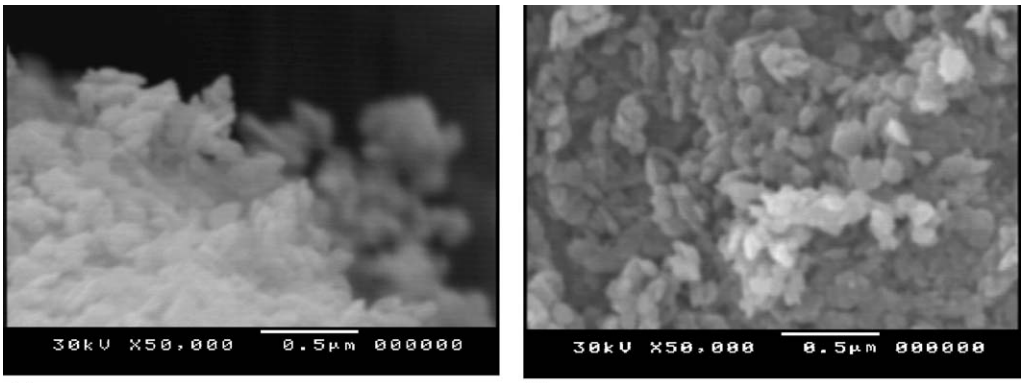

Fig. 1. SEM photographs of $Co(OH)_2$ and CoO: (a) $Co(OH)_2$ precursor and (b) CoO calcinated at 200 °C for 1.0 h.

argon environment described previously [19]. The coin cells were galvanostatically charged and discharged at a suitable *C*-rate.

3. Results and discussion

3.1. Characteristics of $Co(OH)_2$ and CoO

The XRD pattern of $Co(OH)_2$ precipitate prepared by mixing the aqueous solutions of $Co(NO_3)_2$ and NaOH with the aging time over 1 h was compared with the results in the literatures [20,21] to be brucite-like formula (β phase of JCPDS). The grain size of $Co(OH)_2$ calculated from XRD pattern by using the Scherrer equation [22] based on $2\theta = 37.9°$ was 22.9 nm, the BET surface area was obtained to be 28.05 $m^2\,g^{-1}$. A slice-like structure with the particle size of 200 nm was found in the SEM photograph of $Co(OH)_2$ (Fig. 1(a)). A slice structure of CoO calcinated at 200 °C for 1 h was obtained as shown in Fig. 1(b) with the grain size and the BET surface area of 6.59 nm and 89.83 $m^2\,g^{-1}$, respectively [19]. The experimental results indicated that the loss of water from $Co(OH)_2$ to CoO resulted in significant increase in the BET surface area and decrease in the grain size. In the meanwhile the overall surface morphology of CoO was kept the slice-like structure same as the precursor.

3.2. Charge/discharge properties of CoO electrode

The charge/discharge rate (*C*-rate) of Li/CoO coin cell was calculated based on the theoretical discharge capacity of the electroactive material CoO, 715.4 mAh g^{-1} [14]. The charge/discharge curves of CoO electrodes containing 20% carbon black shown in Fig. 2 indicated that the discharge voltage decreased sharply from OCV (2.72 V) to the discharge plateau located in the range of 1.0–0.8 V at the first discharge cycle, and the discharge plateau voltage increased to 1.0–1.4 V for the charge/discharge cycle number of 2. The particle size of CoO calcinated at 200 °C in the range of 0.1–0.3 μm (Fig. 1(b)) was decomposed to be Co and Li_2O with the particle size assumed to be in the range 1–2 nm as reported earlier during the first discharge cycle [14]. The particle size of CoO reproduced in the first charge cycle would be in the similar range of Co and Li_2O

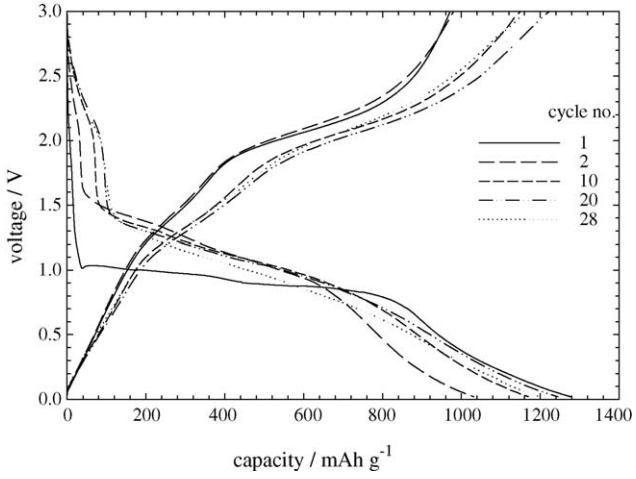

Fig. 2. Charge/discharge curves of Li/CoO (calcinated at 200 °C, 20% carbon black) coin cell. Weight fractions of CoO electrode: CoO (0.6), carbon black (0.2), PVDF (0.2), anode: Li foil, electrolyte: 1.0 M $LiPF_6$ EC–DEC (v/v 1:1) solution, room temperature, potential range of charge/discharge: OCV ~ 0.02 V (first discharge cycle), 3.0–0.02 V (others), charge/discharge rate = 0.1 C.

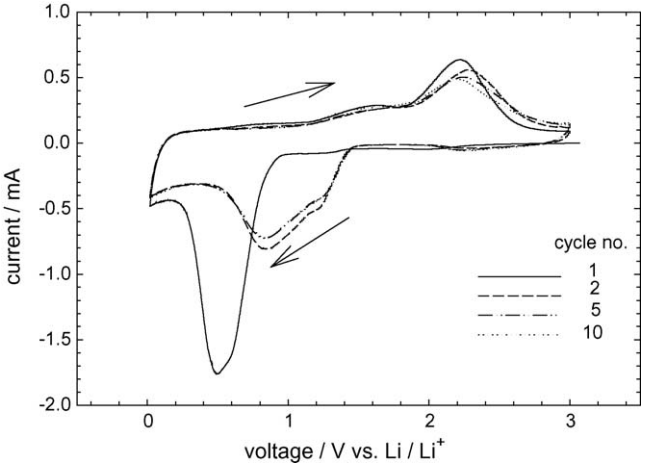

Fig. 3. Cyclic voltammograms of CoO (calcinated at 200 °C) electrode. Weight fractions of CoO electrode: CoO (0.6), carbon black (0.2), PVDF (0.2), weight of CoO = 0.12 mg, anode: Li foil, electrolyte: 1.0 M $LiPF_6$ EC–DEC (v/v 1:1) solution, room temperature, scan range: OCV → 0.02 V → 3.0 V (first cycle), 3.0–0.02 V (2–10 cycles), scan rate = 1 mV s^{-1}.

particles formed in the first discharge cycle, i.e. 1–2 nm. Therefore, comparing with the first discharge cycle, the significant increase in the discharge plateau potential in the second cycle was deduced to be caused by the significant reduction in the particle size of CoO. The charge capacity of Li/CoO increased from 971 to 1237 mAh g^{-1} with increase in the cycle number from 1 to 22 (defined as the activation period), and the charge capacity slightly decreased to 1167.0 mAh g^{-1} for further increase in

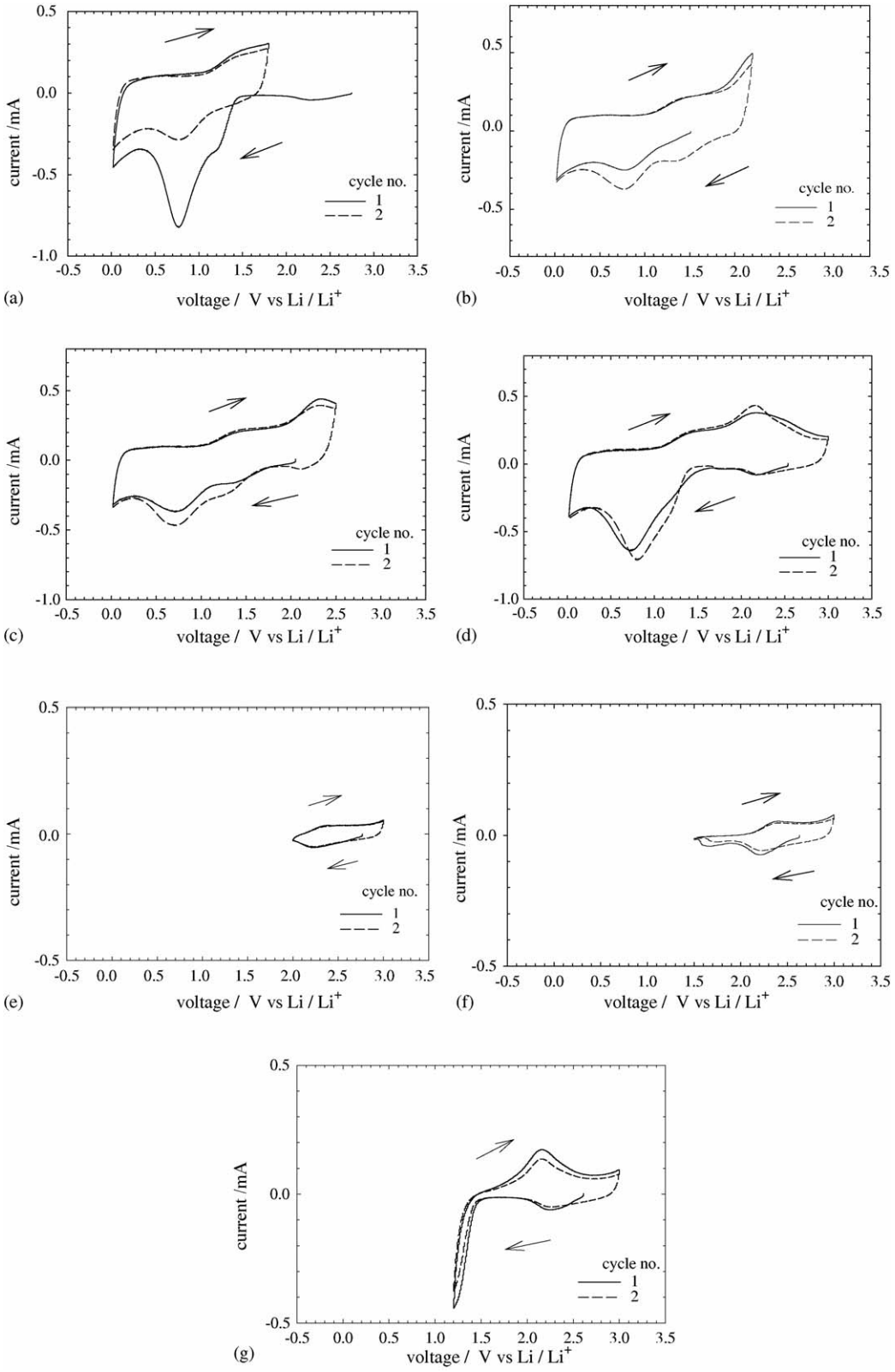

Fig. 4. Cyclic voltammograms of CoO (calcinated at 200 °C) electrode at various scan ranges. Weight fractions of CoO electrode: CoO (0.6), carbon black (0.2), PVDF (0.2), weight of CoO = 0.12 mg, anode: Li foil, electrolyte: 1.0 M $LiPF_6$ EC–DEC (v/v 1:1) solution, room temperature, scan rate = 1 mV s^{-1}.

the cycle number to 28. The activation period was deduced as the cycle number for recovery of the irreversible capacity in the first cycle, which was caused by some of the irreversible Li_2O generated in the first discharge cycle.

The formation of gel-liked polymer (also-called solid-electrolyte interface, SEI) contained LiF, Li_2CO_3 and alkyl-carbonate lithium salts ($ROCO_2Li$) for the potential less than the discharge plateau, e.g. 0.7–0.02 V has been reported in the literatures [23,24]. Some Li^+ were also reduced and stored in the boundary between Co and Li_2O phases for the discharge potential approached to 0 V (versus Li/Li^+), which was extracted for potential range of 0.02–1.1 V in the following charge cycle (Fig. 2). The similar phenomena were studied and demonstrated based on RuO_2 as the anodic material of lithium battery [23]. The main reaction in potential range of 1.1–1.9 V for first charge cycle would be the decomposition of gel-liked polymers. For plateau potential of 1.9–2.5 V in the first cycle of charge process, the reaction was the recombination of Co and Li_2O to produced CoO and Li^+. Furthermore, it was also demonstrated that $LiCoO_2$ could be spontaneously formed in molten carbonate in the presence of CoO, Li^+ and CO_3^{2-} [25,26]. As indicated in Fig. 2, a small discharge plateau found in the potential range of 2.7–2.0 V for the cycle number greater than 2 was deduced to be the intercalation of Li^+ into $LiCoO_2$. The extraction of Li^+ from $LiCoO_2$ would occur for the potential greater than 2.5 V in the charge process (Fig. 2).

3.3. The cyclic voltammograms of CoO electrode

The cathodic reduction current in the first cycle scanned from OCV to 0.02 V was sharply increased for the potential less than 1.0 V, and the cathodic peak current was obtained at potential of 0.5 V (Fig. 3). Two anodic peaks at potentials of 1.5 and 2.4 V were found for scanning reversibly at the first cycle of cyclic voltammetry (CV). Compared with the first cycle, two cathodic peak voltages were found at 1.2 and 0.8 V, respectively, for the second cycle of CV. On the other hand, the anodic peaks changed slightly for the cycle number greater than 2, and the steady cyclic voltammograms were obtained for the cycle number greater than 5.

After CoO electrode was scanned for 10 cycles, CoO electrode was scanned with various scanning ranges as illustrated in Fig. 4. The voltage was scanned at the first cycle from the OCV (2.75 V) to 0.02 V and then scanned reversely to 1.8 V, the cathodic reduction peak currents at 1.2 and 0.8 V were found to be 0.4 and 0.85 mA, respectively (Fig. 4(a)). For the second cycle (voltage range of 1.8–0.02 V), the disappearance of the cathodic peak at 1.2 V and the significant decrease of the cathodic peak current at 0.8 V indicated that the anodic peak corresponded to the cathodic peak at 0.8 V was deduced to be the peak at voltage of 1.5 V (Fig. 3). The redox pair at cathodic and anodic peaks of 0.8 and 1.5 V compared with the charge/discharge curves shown in Fig. 2 was inferred to be the formation and decomposition of the gel-liked polymers. The cathodic peak at 1.5 V appeared again by increasing the scanning right limit at the second cycle from 1.8 to 2.2 V (Fig. 4(b)), and the cathodic peak current increased and gradually merged with the cathodic peak at 0.8 V for further increase in the scanning right limits to 2.5 and 3.0 V (Fig. 4(c) and (d)), respectively. Therefore, the cathodic peak voltage shifted from 1.5 to 1.2 V with the increase in the scanning right limit, and the cathodic peak at 1.2 V was corresponded to the anodic peak voltage of 2.1 V (Fig. 3). The reactions of redox pair for the cathodic and anodic peak voltages at 1.2 and 2.1 V were corresponded to the redox of CoO.

The unknown cathodic peak at 2.2 V shown in Fig. 4(d) was studied by fixing the scanning right limit at 3.0 V and changing the left limits of 2.0, 1.5 and 1.2 V, respectively (Fig. 4(e)–(g)). As shown in Fig. 4(e), a redox pair was found for the cathodic and anodic peaks at 2.2 and 2.3 V, respectively. For increasing the left limit to 1.2 V, the anodic peak at 2.1 V (the anodic oxidation of Co) appeared. Due to the small peak current, the anodic peak at voltage of 2.3 V was then covered by the anodic peak of 2.1 V. According to the discussion about the charge/discharge curves in Fig. 2, the redox pair occurred at 2.2/2.3 V was deduced to be the intercalation and extraction of Li^+ into/from $LiCoO_2$.

4. Conclusions

The precursor of the CoO ($Co(OH)_2$) prepared with the chemical precipitation method by mixing $Co(NO_3)_2$ and NaOH aqueous solutions and aged more than 1 h was identified by XRD to be the brucite-like phase. A slice-like structure with particle size of 200 nm was obtained for $Co(OH)_2$, and the structure and the particle size changed slightly for calcination at 200 °C to obtain CoO. The experimental results indicated that the electrochemical behaviors in the cyclic voltammograms of CoO electrode were correlated well with the charge/discharge curves. The main charge/discharge capacities were contributed from the redox of CoO and the formation/decomposition of gel-like polymers, respectively. The difference in the charge/discharge curve and cyclic voltammogram at the first cycle with the other cycles was deduced to the change in particle size of the electroactive material CoO.

Acknowledgment

The financial support of National Science Council of the Republic of China (Project number: NSC 93-2214-E-029-007), Ministry of Education of Republic of China (Project number: EX-91-E-FA09-5-4) and Tunghai University is acknowledged.

References

[1] Y. Idota, T. Kubota, A. Matsufuji, Y. Maekawa, T. Miyasaka, Science 276 (1997) 1395.
[2] I.A. Courtney, J.R. Dahn, J. Electrochem. Soc. 144 (1997) 2045.
[3] J. Read, D. Foster, J. Wolfenstine, W. Behl, J. Power Sources 96 (2001) 277.
[4] F. Belliard, J.T.S. Irvine, J. Power Sources 97–98 (2001) 219.
[5] F. Badway, I. Plitz, S. Grugeon, S. Laruelle, M. Dollé, A.S. Gozdz, J.-M. Tarascon, Electrochem. Solid-State Lett. 5 (2002) 115.
[6] G.X. Wang, Y. Chen, K. Konstantinov, J. Yao, J. Shn, H.K. Liu, S.X. Dou, J. Alloys Compd. 340 (2002) L5.

[7] G.X. Wang, Y. Chen, K. Konstantinov, M. Lindsay, H.K. Liu, S.X. Dou, J. Power Sources 109 (2002) 142.
[8] D. Larcher, G. Sudant, J.-B. Leriche, Y. Chabre, J.-M. Tarascon, J. Electrochem. Soc. 149 (2002) A234.
[9] Y.-M. Kang, K.-T. Kim, K.-Y. Lee, S.-J. Lee, J.-H. Jung, J.-Y. Lee, J. Electrochem. Soc. 150 (2003) A1538.
[10] S. Denis, E. Baudrin, M. Touboul, J.-M. Tarascon, J. Electrochem. Soc. 144 (1997) 4099.
[11] E. Baudrin, S. Laruelle, S. Denis, M. Touboul, J.-M. Tarascon, Solid State Ionics 123 (1999) 139.
[12] S. Denis, E. Baudrin, F. Orsini, G. Ouvrard, M. Touboul, J.-M. Tarascon, J. Power Sources 81–82 (1999) 79.
[13] S. Laruelle, P. Poizot, E.N. Baudrin, V. Briois, M. Touboul, J.-M. Tarascon, J. Power Sources 97–98 (2001) 251.
[14] P. Poizot, S. Laruelle, S. Grugeon, L. Dupont, J.-M. Tarascon, Nature 407 (2000) 496.
[15] S. Grugeon, S. Laruelle, R. Herrera-Urbina, L. Dupont, P. Poizot, J.-M. Tarascon, J. Electrochem. Soc. 148 (2001) A285.
[16] S. Grugeon, S. Laruelle, P. Poizot, J.-M. Tarascon, US Patent WO 200,171,833 (2001).
[17] S. Laruelle, S. Grugeon, P. Poizot, M. Dollé, L. Dupont, J.-M. Tarascon, J. Electrochem. Soc. 149 (2002) A627.
[18] M. Dollé, P. Poizot, L. Dupont, J.-M. Tarascon, Electrochem. Solid-State Lett. 5 (2002) A18.
[19] J.S. Do, C.H. Weng, J. Power Sources 146 (2005) 482.
[20] Z.P. Xu, H.C. Zeng, J. Mater. Chem. 8 (1998) 2499.
[21] Z.P. Xu, H.C. Zeng, Chem. Mater. 11 (1999) 67.
[22] C. Lin, J.A. Ritter, B.N. Popov, J. Electrochem. Soc. 145 (1998) 4097.
[23] P. Balaya, H. Li, L. Kienle, J. Maier, Adv. Funct. Mater. 13 (2003) 621.
[24] R. Dedryve‘re, S. Laruelle, S. Grugeon, P. Poizot, D. Gonbeau, J.-M. Tarascon, Chem. Mater. 16 (2004) 1056.
[25] P. Tomczyk, H. Sato, K. Yamada, T. Nishina, I. Uchida, J. Electroanal. Chem. 391 (1995) 133.
[26] P. Tomczyk, M. Mosialek, J. Oblakowski, Electrochim. Acta 47 (2001) 945.